

The Physics Case for an e^+e^- Linear Collider

James E. Brau^a, Rohini M. Godbole^b, Francois R. Le Diberder^c, M.A. Thomson^d,
Harry Weerts^e, Georg Weiglein^f, James D. Wells^g, Hitoshi Yamamoto^h

A Report Commissioned by the Linear Collider Community[†]

(^a) Center for High Energy Physics, University of Oregon, USA

(^b) Centre for High Energy Physics, Indian Institute of Science, Bangalore, India

(^c) Laboratoire de l'Accélérateur Linéaire, IN2P3/CNRS et Université Paris-Sud, France

(^d) Cavendish Laboratory, University of Cambridge, UK

(^e) Argonne National Laboratory, Argonne, USA

(^f) DESY, Hamburg, Germany

(^g) CERN, Geneva, Switzerland

(^h) Tohoku University, Japan

1 Introduction

The physics motivation for an e^+e^- linear collider (LC) has been studied in detail for more than 20 years. These studies have provided a compelling case for a LC as the next collider at the energy frontier. The unique strengths of a LC stem from the clean experimental environment arising from e^+e^- collisions. In particular, the centre-of-mass energy and initial-state polarisations are precisely known and can be adjusted, and backgrounds are orders of magnitude lower than the QCD backgrounds that challenge hadron collider environments. The low backgrounds permit trigger-free readout, and the measurements and searches for new phenomena are unbiased and comprehensive. These favourable experimental conditions will enable the LC to measure the properties of physics at the TeV scale with unprecedented precision and complementarity to the LHC. The observation at the LHC of a new particle compatible with a light Higgs boson strengthens the physics case for a LC even more.

The main goals of the LC physics programme are:

- precise measurements of the properties of the Higgs sector;
- precise measurements of the top quark and gauge sector;
- searches for physics beyond the Standard Model (SM), where, in particular, the discovery reach of the LC can significantly exceed that of the LHC for the pair-production of colour-neutral states; and
- sensitivity to new physics through tree-level exchanges or quantum effects in high-precision observables.

The complementarity of the LC and LHC has been established over many years by a dedicated worldwide collaborative effort. It has been shown in many contexts that for new particles found at the LHC, the LC will be essential in determining the properties of these new particles and unraveling the underlying structure of the new physics.

The development of the SM was a triumph for modern science. The experimental confirmation of the $SU(3)_C \times SU(2)_L \times U(1)_Y$ gauge structure of the SM and the precise measurement of its parameters were achieved through a combination of analyses from electron-positron and hadron colliders, such as LEP, SLC,

[†]See Addendum for this committee's origin and charge.

39 HERA, B-factories and the Tevatron. These precision measurements are compatible with the minimal Brout-
40 Englert-Higgs mechanism of Electroweak Symmetry Breaking (EWSB), through which the masses of all
41 the known fundamental particles are generated. The measurements of electroweak precision observables
42 show a pronounced preference for a relatively low-mass SM Higgs boson.

43 The observation of a new particle compatible with a Higgs boson of mass ~ 125 GeV is a major break-
44 through in particle physics. It represents one of the most significant discoveries of modern science. Given
45 the far-reaching consequences for our understanding of the fundamental structure of matter and the basic
46 laws of nature, it is of the highest priority to probe the properties of this particle to address such questions
47 as:

- 48 • What is the mass and quantum numbers of this particle?
- 49 • What are the couplings of this particle to other known elementary particles? Is its coupling to each
50 particle proportional to that particle's mass, as required in the SM by the Higgs mechanism?
- 51 • Is this particle a single, fundamental scalar as in the SM, or is it part of a larger structure? Is it part of
52 a model with additional scalar doublets? Or, could it be a composite state, bound by new interactions?
- 53 • Does this particle couple to new particles with no other couplings to the SM? Is the particle mixed
54 with new scalars of exotic origin, for example, the radion of extra-dimensional models?
- 55 • What is the value of the particle's self-coupling? Is this consistent with the expectation from the
56 symmetry breaking potential?

57 The LC provides a unique opportunity to study Higgs properties with sufficient precision to answer these
58 fundamental questions. The large numbers of Higgs bosons that would be produced at a LC, between 10^5
59 and 10^6 depending on centre-of-mass energy and integrated luminosity, and the clean final states mean
60 that a LC can be considered as a Higgs factory where the properties of the Higgs boson can be studied in
61 great detail. In particular, a LC provides the possibility of model-independent measurements of the Higgs
62 couplings to the gauge bosons and fermions at the 1 – 5% level. According to current knowledge, the
63 expected precision at the LHC, even after the high-luminosity upgrade, is significantly worse and without
64 further theoretical assumptions only ratios of couplings can be determined.

65 Whilst the discovery of a signal compatible with a Higgs boson at the LHC represents a breakthrough in
66 particle physics, it should be kept in mind that the minimal EWSB theory of the SM without other dynamical
67 mechanisms has theoretical shortcomings, and a richer and more complex structure is generally favoured.
68 Most of the ideas for physics beyond the SM (BSM) are driven by the need to achieve a deeper understanding
69 of the EWSB mechanism, thus the confirmation of a Higgs signal has far-reaching consequences. Further-
70 more, the presence of non-baryonic dark matter in the cosmos is an experimentally established fact that
71 implies BSM physics. To date, no clear sign of BSM physics has emerged from LHC data. For new states
72 that are colour-neutral, a LC provides sensitivity for direct discovery via pair production. This complements
73 the search reach of the LHC, where the highest sensitivity is achieved for BSM coloured states. For exam-
74 ple, in the context of SUSY, a LC would provide the potential for both discovery and precise measurements
75 of the properties of the electroweak gaugino sector, the superpartners of the leptons and the additional states
76 of an extended Higgs sector that are generally much lighter than the coloured superpartners. Should the two
77 machines be operating concurrently, the LC results could even provide feed-back to the LHC experiments
78 and vice versa.

79 The flexibility of the LC will give rise to a rich physics programme which could consist of i) a low-
80 energy phase with \sqrt{s} in the range of 250 – 500 GeV, encompassing the possible ZH, $t\bar{t}$, HHZ and $t\bar{t}H$
81 thresholds, and ii) a high-energy phase with $\sqrt{s} > 500$ GeV allowing a high statistics study of the Higgs
82 boson through the WW fusion process and allowing access to rarer Higgs production processes such as
83 $e^+e^- \rightarrow HH\nu_e\bar{\nu}_e$. The precise centre-of-mass energy range for the higher energy operation would be set
84 by the BSM physics scale, where the flexibility in energy of a LC would allow the threshold behaviour

85 for any new physics process to be mapped out in detail. While this document focuses on the minimal LC
86 programme, there are a number of optional phases of LC operation, like GigaZ, which is a high-luminosity
87 Z-factory, and $e\gamma$ and $\gamma\gamma$ configurations.

88 Two options for a future e^+e^- LC have been developed, with different main linac acceleration schemes.
89 The International Linear Collider (ILC) uses superconducting RF, whereas the Compact Linear Collider
90 (CLIC) uses a separate drive beam to provide the accelerating power. The ILC technology is mature and
91 provides an option for a Higgs and top factory to be constructed on a relatively short timescale. The CLIC
92 technology requires further R&D but provides the potential to reach higher centre-of-mass energies. In
93 recent years there has been extensive collaboration between ILC and CLIC physicists with the goal of re-
94 alising a LC as the next major new facility. Furthermore, the ILC and CLIC studies are being organised
95 under the same formal worldwide body, the Linear Collider Board (LCB) reporting directly to ICFA. The
96 strong accelerator development programme is complemented by an active theory and experimental commu-
97 nity working on the physics and detectors for a future LC. These studies have resulted in detailed designs
98 for the detectors at a LC, and, based on detailed simulation studies, have provided a clear demonstration
99 that the LC physics goals can be achieved. The main results from these physics studies are summarised
100 below within the context of the results that have been obtained at the LHC up to now and with a view also
101 to the possible progress from the running of the LHC during the next years. Unless otherwise stated, the
102 discussion refers generically to a Linear Collider (LC) rather than to the specific realisations ILC or CLIC.

103 A comprehensive review of LC physics has been given in the Physics volume of the ILC RDR report [8].
104 More recently, many important measurement at the ILC and CLIC have been analysed in full-simulation
105 studies with fully realised model detectors. These results are reported in [9], [10], and [11]. Finally, new
106 reports on LC physics have attempted to bring the discussion of the LC capabilities up to date in relation to
107 recent results from the LHC. These reports can be found in [11] and [13]. This document will summarise
108 important results presented more fully in these references.

109 **2 Higgs Physics and Electroweak Symmetry Breaking**

110 In the SM, the Higgs boson plays a special role. The Higgs mechanism is responsible for electroweak
111 symmetry breaking and accounts for the generation of the masses of all the other elementary particles. In
112 order to distinguish a SM Higgs from possible alternative scenarios, it is necessary to measure precisely its
113 couplings to the gauge bosons and the fermions. Furthermore, the spin and the CP-properties of the new
114 state need to be determined, and it must be clarified whether there is more than one physical Higgs boson.
115 At the LHC ratios of the Higgs couplings to different particles can be measured for a subset of the possible
116 decays. Earlier studies [1] suggest that even with 3000 fb^{-1} of data the precision achievable is somewhat
117 limited, $\Gamma_W/\Gamma_Z \sim 10\%$, $\Gamma_W/\Gamma_t \sim 10\%$, $\Gamma_W/\Gamma_b \sim 25\%$ and $\Gamma_W/\Gamma_\tau \sim 30\%$. At a LC, the precisions achievable
118 are up to an order of magnitude better than those at the LHC, and a wider range of decay channels can be
119 studied. Furthermore, a LC is the only place where model independent measurements of the Higgs boson
120 couplings can be made.

121 The main strands of the Higgs physics programme at a LC include:

- 122 • Precise measurements of the couplings of the Higgs to the gauge bosons and fermions, and in partic-
123 ular an absolute measurement of its couplings to the Z boson independent of its decay modes;
- 124 • Precise measurements of its mass, width, spin, and CP properties;
- 125 • Measurements of the trilinear Higgs self-coupling, providing direct access to the Higgs potential.

126 A number of these measurements are unique to a LC and the precision achievable significantly surpasses that
127 anticipated at the LHC. The LC measurements would establish whether the Higgs boson has the properties
128 predicted by the SM, or is part of an extended Higgs sector such as in SUSY models, or whether it has a
129 completely different physical origin which would be the case for a composite Higgs.

	250 GeV	350 GeV	500 GeV	1 TeV	1.5 TeV	3 TeV
$\sigma(e^+e^- \rightarrow ZH)$	240 fb	129 fb	57 fb	13 fb	6 fb	1 fb
$\sigma(e^+e^- \rightarrow H\nu_e\bar{\nu}_e)$	8 fb	30 fb	75 fb	210 fb	309 fb	484 fb
Int. \mathcal{L}	250 fb^{-1}	350 fb^{-1}	500 fb^{-1}	1000 fb^{-1}	1500 fb^{-1}	2000 fb^{-1}
# ZH events	60,000	45,500	28,500	13,000	7,500	2,000
# $H\nu_e\bar{\nu}_e$ events	2,000	10,500	37,500	210,000	460,000	970,000

Table 1: The leading-order Higgs cross sections for the Higgs-strahlung and WW-fusion processes at various centre-of-mass energies for $m_H = 125$ GeV. Also listed the expected number of events accounting for the anticipated luminosities obtained from approximately 5 years running at these energies.

\sqrt{s}	250 GeV	350 GeV
Int. \mathcal{L}	250 fb^{-1}	350 fb^{-1}
$\Delta(\sigma)/\sigma$	3 %	4 %
$\Delta(g_{HZZ})/g_{HZZ}$	1.5 %	2 %

Table 2: Precision measurements of the Higgs coupling to the Z at $\sqrt{s} = 250$ GeV and $\sqrt{s} = 350$ GeV based on full simulation studies with $m_H = 120$ GeV. Results from [10] and follow-up studies.

2.1 Higgs Production at a Linear Collider

At a LC, the main Higgs production channels are through the Higgs-strahlung and vector boson fusion processes. At relatively low centre-of-mass energies the Higgs-strahlung process, $e^+e^- \rightarrow ZH$, dominates, with a peak cross section at approximately 30 GeV above the ZH production threshold. At higher centre-of-mass energies, the WW fusion process $e^+e^- \rightarrow H\nu_e\bar{\nu}_e$ becomes increasingly important. For a low mass Higgs boson the fusion process dominates above $\sqrt{s} \sim 500$ GeV. The WW fusion cross section increases approximately logarithmically with \sqrt{s} , allowing large samples of Higgs bosons to be studied at a TeV-scale LC. The ZZ fusion process $e^+e^- \rightarrow H\nu_e\bar{\nu}_e$ has a cross section which is approximately an order of magnitude smaller than the WW fusion process. Table 1 compares the expected number of ZH and $H\nu_e\bar{\nu}_e$ at the main centre-of-mass energies considered in the ILC and CLIC studies. Even at the lowest LC energies considered, large samples of Higgs bosons can be accumulated. In addition to the main Higgs production processes, rarer processes such as $e^+e^- \rightarrow t\bar{t}H$, $e^+e^- \rightarrow ZHH$ and $e^+e^- \rightarrow HH\nu_e\bar{\nu}_e$ provide access to the top quark Yukawa coupling and the Higgs trilinear self-coupling.

2.2 Higgs Coupling Measurements at $\sqrt{s} < 500$ GeV

The Higgs-strahlung process provides the opportunity to study the couplings of the Higgs boson in a *model-independent* manner. This is unique to a LC. The clean experimental environment and the relatively low SM cross sections for background processes, allow $e^+e^- \rightarrow ZH$ events to be selected based on the identification of two opposite charged leptons with invariant mass consistent with m_Z . The remainder of the event, i.e. the Higgs decay, is not considered in the event selection. For example, Figure 1 shows the simulated invariant mass distribution of the system recoiling against identified $Z \rightarrow \mu^+\mu^-$ decays at a LC for $\sqrt{s} = 250$ GeV. A clear peak at the generated Higgs mass of $m_H = 120$ GeV is observed. Because only the properties of the di-lepton system are used in the selection, this method provides an absolute measurement of the Higgs-strahlung cross section, regardless of the Higgs boson decay modes; it would be equally valid if the Higgs boson decayed to invisible final states. Hence a model-independent measurement of the coupling g_{HZZ} can be made. The precisions achievable on the Higgs-strahlung cross section and the coupling g_{HZZ} are shown in Table 2 for $m_H = 120$ GeV.

The recoil mass study provides an absolute measurement of the total ZH production cross section and

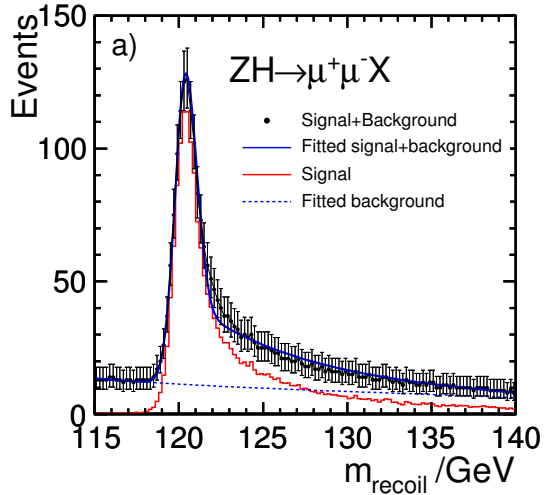


Figure 1: The recoil mass distribution for $e^+e^- \rightarrow ZH \rightarrow \mu^+\mu^-H$ events with $m_H = 120$ GeV in the ILD detector concept at the ILC [10]. The numbers of events correspond to 250 fb^{-1} at $\sqrt{s} = 250$ GeV, and the error bars show the expected statistical uncertainties on the individual points.

157 therefore the total number of Higgs bosons produced would be known with a statistical precision of 3 –
 158 4%. The systematic uncertainties from the knowledge of the integrated luminosity and event selection
 159 are expected to be significantly smaller. Subsequently, by identifying the individual final states for different
 160 Higgs and Z decay modes, absolute measurements of the Higgs boson branching fractions can be made. Due
 161 to the clean final states and the low levels of machine background at a LC, high flavour tagging efficiencies
 162 are achievable and the $H \rightarrow b\bar{b}$, $H \rightarrow c\bar{c}$ and $H \rightarrow g\bar{g}$ decays can be separated. Table 3 summarises the
 163 branching fraction precisions achievable at a LC collider operating at either 250 GeV or 350 GeV where
 164 model-independent measurements of the Higgs boson couplings to the b-quark, c-quark, τ -lepton, W-boson
 165 and Z-boson can be made to better than 5%. There are ongoing studies of how well the top Yukawa
 166 coupling can be measured at a 500 GeV and 1 TeV LC. Preliminary results indicate that a precision of
 167 $\Delta g_{tH}/g_{tH} \sim 10\%$ can be achieved.

168 2.3 Higgs Coupling Measurements at $\sqrt{s} \geq 500$ GeV

169 For a light Higgs boson, at centre-of-mass energies above 500 GeV the WW fusion process, $e^+e^- \rightarrow H\nu_e\bar{\nu}_e$,
 170 becomes the largest single source of Higgs bosons at a future LC, giving rise to event samples of between
 171 $\sim 10^5 - 10^6$ Higgs bosons as indicated in Table 1. Although Higgs production via the ZZ fusion process is
 172 suppressed by about one order of magnitude relative the WW fusion process, the cross section is significant.
 173 For example, at CLIC operating at 3 TeV and $m_H \sim 125$ GeV, approximately $10^5 e^+e^- \rightarrow H\nu_e\bar{\nu}_e$ events
 174 would be produced leading to a measurement of the relative couplings of the Higgs boson to the W and Z
 175 at the 1% level. This would provide a strong test of the SM prediction $g_{HWW}/g_{HZZ} = \cos^2 \theta_W$.

176 The ability for clean flavour tagging combined with the large samples of WW fusion events, allows
 177 the production rate of $e^+e^- \rightarrow H\nu_e\bar{\nu}_e \rightarrow b\bar{b}\nu_e\bar{\nu}_e$ to be determined with a precision of better than 1%.
 178 Furthermore, the couplings to the fermions can be measured more precisely at high energies, even when
 179 accounting for the uncertainties on the production process. For example, Table 3 shows the precision on the
 180 branching ratio obtained from full simulation studies as presented in [11]. The absolute uncertainties on the
 181 Higgs couplings can be obtained by combining the high energy results with those from the Higgs-strahlung
 182 process. The high statistics Higgs samples would allow for very precise measurements of relative branching
 183 ratios. For example, a LC operating at 3 TeV would give a statistical precision of 1.5% on g_{Hcc}/g_{Hbb} .

	250 GeV	350 GeV	3 TeV		250 GeV	350 GeV	3 TeV
$\sigma \times Br(H \rightarrow bb)$	1.0 %	1.0 %	0.2 %	g_{Hbb}	1.6 %	1.4 %	2 %
$\sigma \times Br(H \rightarrow cc)$	8 %	6 %	3 %	g_{Hcc}	4 %	3 %	2 %
$\sigma \times Br(H \rightarrow \tau\tau)$	6 %*	6 %	?	$g_{H\tau\tau}$	3 %*	3 %	?
$\sigma \times Br(H \rightarrow WW)$	8 %	6 %	?	g_{HWW}	4 %	3 %	< 2 %
$\sigma \times Br(H \rightarrow \mu\mu)$	–	–	15 %	$g_{H\mu\mu}$	–	–	7.5 %
$\sigma \times Br(H \rightarrow gg)$	9 %	7 %	?	g_{HWW}/g_{HZZ}	?	?	< 1 %*

Table 3: The precision on the Higgs branching ratios and couplings obtainable from studies of the Higgs-strahlung process at a LC operating at either $\sqrt{s} = 250$ GeV or $\sqrt{s} = 350$ GeV for respective integrated luminosities of 250 fb^{-1} and 350 fb^{-1} . The uncertainties on the couplings include the uncertainties on g_{HZZ} obtained from the absolute measurement of the ZH cross section. Also shown are the precisions achievable from the WW fusion process at a LC operating at 3 TeV. The numbers marked with asterisk are estimates, all other numbers come from full simulation studies with $m_H = 120$ GeV. The question marks indicate that the results of ongoing studies are not yet available. In all cases the luminosities assumed are those given in Table 1.

184 2.4 Higgs Self-Coupling

In the SM, the Higgs boson originates from a doublet of complex scalar fields described by the potential

$$V(\phi) = \mu^2 \phi^\dagger \phi + \lambda (\phi^\dagger \phi)^2.$$

185 After spontaneous symmetry breaking, this form of the potential gives rise to a triple Higgs coupling of
186 strength proportional to λv , where v is the vacuum expectation value of the Higgs potential. The mea-
187 surement of the strength of the Higgs trilinear self-coupling therefore provides direct access to the quartic
188 potential coupling λ assumed in the Higgs mechanism. This measurement is therefore crucial for experi-
189 mentally establishing the Higgs mechanism. For a low-mass Higgs boson, the measurement of the Higgs
190 boson self-coupling at the LHC will be extremely challenging even with 3000 fb^{-1} of data. At an e^+e^- LC,
191 the Higgs self-coupling can be measured through the $e^+e^- \rightarrow ZHH$ and $e^+e^- \rightarrow HH\nu_e\bar{\nu}_e$ processes [2].
192 The precision achievable is currently being studied for the $e^+e^- \rightarrow ZHH$ process at $\sqrt{s} = 500$ GeV and
193 for the $e^+e^- \rightarrow HH\nu_e\bar{\nu}_e$ process at $\sqrt{s} > 1$ TeV. Given the complexity of the final state and the smallness
194 of the cross sections, these studies are being performed with a full simulation of the LC detector concepts.
195 The preliminary results indicate that a precision of $\lesssim 20\%$ on λ is achievable, with the greatest sensitivity
196 coming from $e^+e^- \rightarrow HH\nu_e\bar{\nu}_e$.

197 2.5 Total Higgs Width

For Higgs boson masses below 140 GeV, the total Higgs decay width in the SM (Γ_H) is less than 10 MeV and cannot be measured directly. Nevertheless, at a LC Γ_H can be determined from the relationship between the total and partial decay widths, for example

$$\Gamma_H = \Gamma(H \rightarrow WW^*)/Br(H \rightarrow WW^*).$$

198 Here $\Gamma(H \rightarrow WW^*)$ can be determined from the measurement of the HWW coupling obtained from the
199 fusion process $e^+e^- \rightarrow H\nu_e\bar{\nu}_e$. When combined with the direct measurement of $Br(H \rightarrow WW^*)$, this
200 allows the Higgs width to be inferred. Alternatively, the model-independent measurement of the HZZ cou-
201 pling, which is sensitive to invisible and undetectable decay modes, can be used exploiting SU(2) invariance
202 ($g_{HWW}/g_{HZZ} = \cos \theta_W$) which can be established at a LC. With either approach a precision on the total
203 decay width of the Higgs boson of about 6% at $\sqrt{s} = 500$ GeV can be reached. This improves to better than
204 4% at 1 TeV.

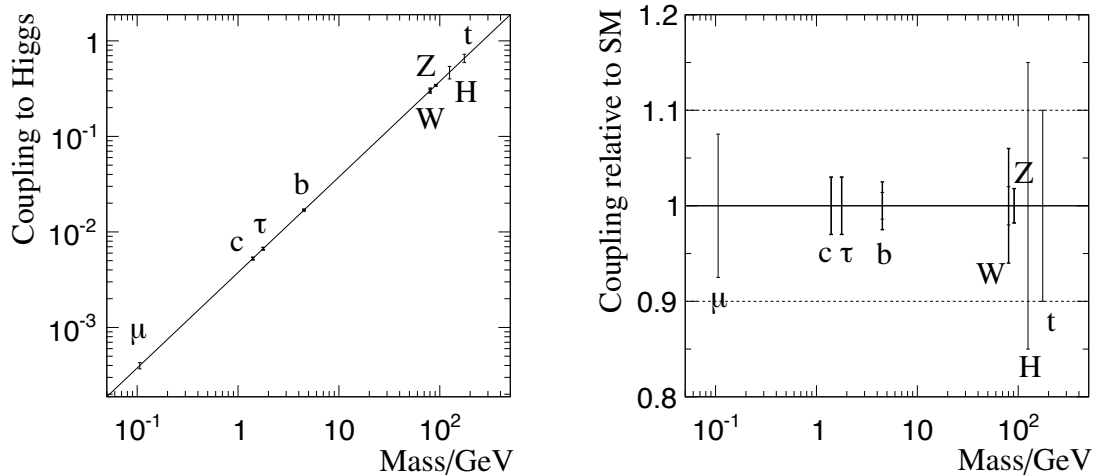


Figure 2: An illustration of the typical precisions to which the relation between the Higgs couplings to the masses of the particles can be tested at a linear collider, assuming operation at one energy point below and one above $\sqrt{s} = 500$ GeV with the integrated luminosities of Table 1. The ultimate sensitivity will depend on the precise integrated luminosity recorded and the centre-of-mass energies at which the LC is operated. The two plots show the absolute and relative precision that can be reached. The values shown assume SM couplings.

205 2.6 Impact of the Precision Measurements of the Higgs Couplings

206 Whilst the precise measurements of the Higgs couplings to gauge bosons and fermions possible at a LC are
 207 of interest in their own right, they will be crucial for testing the fundamental prediction of the Higgs mech-
 208 anism that the Higgs coupling to different particles is proportional to masses, as summarised in Figure 2.

209 After the discovery of the Higgs boson, the precise measurements at a LC will provide a powerful probe
 210 of the structure of the Higgs sector. The SM with a single Higgs doublet is only one of many possibilities.
 211 The model-independent measurements at a LC will be crucial to distinguish between the different possible
 212 manifestations of the underlying physics. It is a general property of many extended Higgs theories that the
 213 lightest Higgs scalar can have nearly identical properties to the SM Higgs boson. In this so-called decoupling
 214 limit, additional states of the Higgs sector are heavy and may be difficult to detect both at the LHC and LC.
 215 Thus, precision measurements are crucial in order to distinguish the simple Higgs sector of the SM from a
 216 more complicated scalar sector. Deviations from the SM can arise from an extended structure of the Higgs
 217 sector, for instance if there are more than one Higgs doublet. Another source of possible deviations from
 218 the SM Higgs properties are loop effects from BSM particles. The potential for deciphering the physics of
 219 EWSB is directly related to the sensitivity for verifying deviations from the SM. For example, in Figure 3 the
 220 typical deviations from the SM predictions for a Two-Higgs-Doublet model are compared to the precision
 221 on the couplings achievable at a LC. In this example, the high-precision measurements at the LC would
 222 clearly indicate the non-SM nature of the EWSB sector.

223 Furthermore, small deviations from SM-like behaviour can arise as a consequence of fundamentally
 224 different physics of electroweak symmetry breaking. For example, if an additional fundamental scalar such
 225 as the radion is present, the ratios of branching ratios may be unchanged but the total decay rate is reduced.
 226 In this case only the high-precision and model-independent measurements of couplings from a LC would
 227 establish a deviation from the SM.

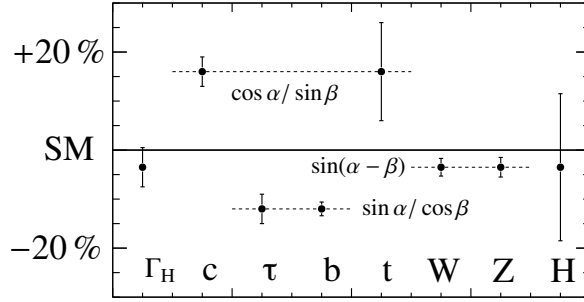


Figure 3: Typical deviations of the Higgs couplings to different particles from the SM predictions in a Two-Higgs-Doublet model. The LC precisions for the various couplings are the same as in Figure 2.

2.7 Higgs Boson Mass, Spin and CP Properties

A LC is the ideal place to measure the properties of the Higgs boson. For example, the mass of the Higgs boson can be determined at a LC with a precision of better than 50 MeV, either from the recoil mass distribution at $\sqrt{s} = 250$ GeV or from the direct reconstruction of its decay products. This would improve on the precise measurement obtained from the $\gamma\gamma$ decay mode at the LHC.

Information about the spin of the Higgs boson can be obtained through the Higgs-strahlung process from the threshold dependence of the cross section as well as angular distributions of the Z and its decay products. For example, Figure 4 shows the precision obtained from a threshold scan with an integrated luminosity of just 20 fb^{-1} at each point which is sufficient to establish the spin of the Higgs boson. Although the measurement of the Higgs boson spin can also be performed at the LHC, a LC provides a unique window into the possibility of CP violation in the Higgs and top sector. Furthermore, the energy dependence of the Higgs-strahlung cross section in the SM contains a factor β , whereas for a CP-odd Higgs boson with $J^{PC} = 0^{+-}$, the corresponding factor would be β^3 . Again the threshold behaviour of the cross section can differentiate between the two spin-0 cases.

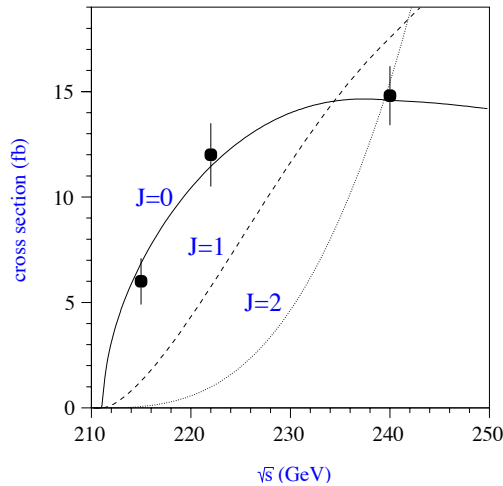


Figure 4: The $e^+e^- \rightarrow ZH$ cross section energy dependence near threshold for different spin states, assuming $m_H = 120$ GeV.

Angular correlations in $e^+e^- \rightarrow HZ \rightarrow 4f$ as well as $H \rightarrow \tau^+\tau^-$ decays are also sensitive to the CP nature of the Higgs state. Since *a priori* the observed Higgs state can be an admixture of CP even and CP odd states, the determination of the CP properties is experimentally more challenging than the measurement

of spin of the Higgs boson. For a Higgs boson, Φ , the most general model independent expression for the ΦVV vertex can be written as

$$g_{\Phi VV} = -gM_V \left[\alpha g^{\mu\nu} + \beta (p \cdot q g_{\mu\nu} / M_V^2 - p_\nu q_\mu) + i \gamma / M_V^2 \epsilon_{\mu\nu\rho\sigma} p^\rho q^\sigma \right] \quad (1)$$

where V represents either a W or Z boson and p, q are the four momenta of the two vector bosons. For a SM Higgs $\alpha = 1$ and $\beta = \gamma = 0$. In contrast, for a pure CP odd Higgs boson, $\alpha = \beta = 0$, and γ is expected to be small. A LC provides a unique laboratory to determine α, β and γ and probe the complete tensor structure of the HVV coupling and the CP properties of the Higgs boson. For example, it has been shown that angular observables can be used to measure η , which parameterises the mixing between a CP-even and a CP-odd Higgs state, to an accuracy of 3 – 4 % [2]. The measurements of the CP properties of the Higgs based on the HVV coupling, both at the LHC and a LC, project out the CP-even component of the Higgs and therefore require very large luminosities. A LC is unique in that the measurement of the threshold behaviour of the process $e^+e^- \rightarrow t\bar{t}H$, which depends on the $H\bar{t}t$ coupling, provides an unambiguous determination of the CP of the Higgs boson and provides the potential for a precision measurement of CP-mixing, even when it is small.

3 Top and the Gauge Sector

In addition to the precision studies in the Higgs sector, a further important part of the programme is establishing the detailed profile of the top quark and studying the gauge sector with high precision, to seek answers to fundamental questions about the dynamics of EWSB, and to probe high-scale physics beyond the SM.

3.1 Top Physics

The top quark plays a very special role in the SM. Being the heaviest of the fundamental fermions it is the most strongly coupled to the electroweak symmetry breaking sector and hence intimately related to the dynamics behind the symmetry breaking mechanism. Its large mass affects the prediction for many SM parameters, including the Higgs mass and the W and Z couplings, through radiative corrections. High-precision measurements of the properties and interactions of the top quark can have sensitivity to physics at mass scales much above the electroweak symmetry breaking scale. These studies are therefore a very important laboratory for explorations of the SM and physics beyond it. A LC will have broad capabilities to establish the top quark profile in a precise and model-independent way. Precision knowledge of m_t will play a crucial role in determining the scale Λ up to which the SM can be valid without needing any new physics.

Top Quark Observables

The top mass measurement at the Tevatron has reached an accuracy of about 1 GeV. While the statistics at the LHC will be huge, because of (theoretical) systematic effects, it appears nevertheless questionable whether a further significant improvement of this measurement can be reached. In particular, an important systematic uncertainty is associated with the problem of how to relate the mass parameter that is actually measured at the Tevatron and the LHC to a parameter that is well-defined so that it can be used as an input for theoretical predictions in the SM (or its extensions), such as the \overline{MS} mass. The relation between those parameters is affected by non-perturbative contributions, which can be the limiting factor in further improving the accuracy of the top-quark mass from measurements at hadron colliders. At the LC the measurement of the top-quark mass from the $t\bar{t}$ threshold will be unique since it will enable a high-precision measurement of a “threshold mass”, for which the relation to a well-defined top-quark mass is precisely known and theoretically well under control.

The statistical precision from a threshold scan at the LC with approximately 30 fb^{-1} will be about 20 MeV for the top-quark mass and 30 MeV for the top width. Including the systematic uncertainty from relating the “threshold mass” to the suitable mass parameter of the SM yields an overall precision on m_t

283 of better than 100 MeV, which corresponds to an order of magnitude improvement compared to the mea-
 284 surement at hadron colliders. An alternative way of measuring the top-quark mass at the LC is based on
 285 the invariant-mass distributions of the fully hadronic (bqq bqq) and semi-leptonic ($b\ell\nu bqq$ with $\ell = e, \mu$)
 286 final states. At $\sqrt{s} \sim 500$ GeV and with 500 fb^{-1} , a statistical precision of about 30 MeV can be achieved
 287 from the direct reconstruction of the invariant-mass distributions. These observables in the continuum how-
 288 ever involve systematic uncertainties similar to those mentioned above for the case of the Tevatron and the
 289 LHC. Compared to hadron colliders here one has higher precision on the measured mass parameter and also
 290 smaller theoretical uncertainties in the prediction of the cross-section.

291 *Top-antitop asymmetries*

292 Besides the measurements of the top-quark mass and width, the top physics programme at the LC of-
 293 fers a variety of further observables that have a high sensitivity to potential effects of new physics. Some
 294 interesting examples are the forward-backward asymmetry in top-antitop production, A_{FB} , the beam polari-
 295 sation asymmetry A_{LR} and the polarisation of the top. These asymmetries, are relevant to probe new physics
 296 models that address the issue of fermion mass hierarchy such as the warped extra dimensional models. The
 297 first of these, A_{FB} , has received a lot of attention lately. Both CDF and D0 experiments have reported a
 298 possible deviation of this asymmetry from the SM prediction in $p\bar{p}$ collisions whereas the measurements of
 299 a related asymmetry for the pp initial state at the LHC currently show no significant deviation from the SM
 300 prediction. For the LC, a measurement of A_{FB} was simulated in the SiD LoI using fully hadronic decays and
 301 the ILD LoI using the semileptonic top decays. Due to the clean LC environment accuracies of about 5%
 302 can be achieved which is a significant improvement compared to the expected accuracies at the Tevatron and
 303 the LHC. A 5% measurement of this asymmetry can probe, for example, the Kaluza-Klein (KK) excitation
 304 of the gluons in models with warped extra dimensions, up to a mass of 10–20 TeV.

305 *Couplings to Gauge Bosons*

306 Precise and model-independent measurements at the LC of the top couplings to weak gauge bosons
 307 will be sensitive to interesting sources of non-SM physics, as many models predict anomalous top-quark
 308 couplings [8]. The production of $t\bar{t}$ pairs in e^+e^- collisions and the subsequent decay of the top provide
 309 a sensitive probe of the $t\bar{t}V(V = \gamma, Z)$ vertices. Since the top quark decays before it hadronises, not just
 310 the cross-sections and angular distribution of the produced top, but also various angular distributions of the
 311 decay products of the top, which retain the memory of its polarisation, can be used effectively towards this
 312 end.

The most general expression for the $t\bar{t}Z$ and $t\bar{t}\gamma$ vertex can be written as:

$$\Gamma_{t\bar{t}(\gamma,Z)}^\mu = ie \left\{ \gamma^\mu \left[F_{1V}^{\gamma,Z} + F_{1A}^{\gamma,Z} \gamma^5 \right] + \frac{(p_t - p_{\bar{t}})^\mu}{2 m_t} \left[F_{2V}^{\gamma,Z} + F_{2A}^{\gamma,Z} \gamma^5 \right] \right\}, \quad (2)$$

313 where the only form factors different from zero in the SM are F_{1V}^γ, F_{1V}^Z and F_{1A}^Z . A study of $e^+e^- \rightarrow t\bar{t} \rightarrow$
 314 $\ell^\pm + \text{jets}$ can lead to 1σ sensitivity up to a percent level for all of them at a LC with $\sqrt{s} = 500$ GeV and
 315 luminosities of the order of $100\text{--}200 \text{ fb}^{-1}$ [2]. Use of polarised beams and polarisation asymmetries can
 316 improve matters by providing observables that can disentangle different couplings and also increase the
 317 accuracy at a given luminosity.

The most general tbW coupling can be parameterized in the form

$$\Gamma_{tbW}^\mu = -\frac{g}{\sqrt{2}} V_{tb} \left\{ \gamma^\mu \left[f_1^L P_L + f_1^R P_R \right] - \frac{i\sigma^{\mu\nu}}{M_W} (p_t - p_b)_\nu \left[f_2^L P_L + f_2^R P_R \right] \right\}, \quad (3)$$

318 where $P_{R,L} = \frac{1}{2}(1 \pm \gamma_5)$. In the limit $m_b \rightarrow 0$, f_1^R and f_2^L vanish. In the SM, $f_1^L = 1$ and all other form factors
 319 are zero at tree-level. Measurement of the $t\bar{t}$ production below threshold, assuming that the top width is
 320 measured just to an accuracy of 100 MeV, will allow a measurement of g_{tbW} to a 3% level. With such
 321 precision, a variety of new physics models such as Little Higgs Model or models of top flavour [8] can be
 322 probed, for example, with a simultaneous measurements of $t\bar{t}Z$ axial coupling and left-handed tbW vertex.

323 Use of beam polarisation can even allow probing anomalous effects in the $t\bar{t}g$ system, particularly by testing
 324 symmetries with construction of observables which have specific CP, T transformation properties and are,
 325 eg., T -odd, CP -even or T -odd and CP -odd. It should be noted that the LHC can give an indication of an
 326 anomalous $t\bar{t}g$ coupling through a study of top-quark polarisation in top-pair production, but the LC would
 327 be required to probe the structure in an unambiguous way. Thus the LC can map out the t couplings to all
 328 the gauge bosons in a precise manner which can then be used to probe new physics.

329 **3.2 WW, ZZ Scattering and the Dynamics of Strong Electroweak Symmetry Breaking**

330 Despite the likely perturbative nature of EWSB indicated by the value of the Higgs mass, from both indirect
 331 electroweak precision constraints and direct observation at the LHC, one point is worth remembering. Even
 332 with a light Higgs, there exist formulations of EWSB, such as composite Higgs models, where the light
 333 Higgs boson is part of a larger spectrum of strongly interacting particles, and discernible effects of the
 334 strong dynamics are possible, affecting gauge boson couplings with each other. A careful study of WW/ZZ
 335 scattering and WW final state processes can reveal these effects.

336 The close connection between the WWZ/γ vertices and restoration of unitarity at high energies in
 337 W^+W^- pair production in e^+e^- collision means that this process is highly sensitive to the triple-gauge-boson
 338 vertices and to heavy resonances with mass far exceeding the LC energy. Further, the same connection un-
 339 derlies the importance of this measurement to look for footprints of any new physics. The most general
 340 WWV interactions with ($V = Z/\gamma$) consistent with Lorentz symmetry, involve twelve (six each for the γ
 341 and the Z) independent couplings, out of which only four have nonzero values in the SM. Terms involving
 342 different couplings are characterised by different tensor structures and different momentum dependencies.
 343 Specific models of the strong dynamics have specific predictions for some of the anomalous couplings.

344 These different kinds of couplings can be disentangled from each other using production angle distribu-
 345 tions and decay product angular distributions, the latter being decided by the polarisation of the produced
 346 W . High beam polarisations (both e^- and e^+) can be used effectively to probe these. An analysis using a
 347 fast simulation performed at the two energies $\sqrt{s} = 500$ GeV and 800 GeV [5, 8] shows that deviations of
 348 all these couplings from their SM values can be measured to better than one per mil level with luminosities
 349 up to 1 ab^{-1} . In many cases the measurements are competitive or do up to an order of magnitude better than
 350 the capabilities of a 14 TeV LHC that had been projected [5, 8].

A chiral Lagrangian for EWSB has numerous operators that govern the interactions of the vector boson
 degrees of freedom. One example is

$$\Delta L = e\kappa_\gamma W_\mu^\dagger W_\nu F^{\mu\nu} \quad \text{where} \quad 1 - \kappa_\gamma = \begin{cases} 0, & \text{Standard Model Higgs Theory} \\ \sim 0.003, & \text{Minimal Strong Coupling Theory} \end{cases}$$

351 This small shift in κ_γ yields a measurable contribution to the anomalous magnetic moment of the W boson,
 352 which is marginal for the LHC to discern but readily observable at a 500 GeV LC [3].

353 The above is an example of deviations in the triple-gauge-boson vertices due to strong dynamics in the
 354 EWSB sector. There are also deviations in quartic boson interactions, which directly affect pure gauge boson
 355 scattering through local contact interactions, such as $WW \rightarrow WW$. The processes $e^+e^- \rightarrow \nu_e\bar{\nu}_e W^+W^- \rightarrow$
 356 $\nu_e\bar{\nu}_e jjjj$ and $e^+e^- \rightarrow \nu_e\bar{\nu}_e ZZ \rightarrow \nu_e\bar{\nu}_e jjjj$ have been studied for LC at $\sqrt{s} = 1$ TeV with 1 ab^{-1} of integrated
 357 luminosity [10], with a view to study these anomalous quartic vertices. The LC sensitivity is comparable
 358 to the values predicted in models of strong dynamics in the EW sector, where the non-SM operators are
 359 constrained to be consistent with the EW precision tests. These measurements require study of angular
 360 correlations among the decay products of the W/Z and further needs separation of the W and Z final states
 361 decaying to quarks. This indeed has been a benchmark requirement, which has driven the need for excellent
 362 jet-energy resolution, which in turn has driven the design of LC detector concepts and has been shown to be
 363 achievable.

As mentioned above, one could have strong dynamics at the origin of EWSB, even for a light Higgs
 boson, and it could be a composite particle remnant. In the case of these composite Higgs models, the

Lagrangian of the Higgs boson interactions with the vector bosons can be parameterized as

$$\Delta L = \left(m_W^2 W_\mu^+ W^{\mu-} + \frac{m_Z^2}{2} Z_\mu Z^\mu \right) \left[1 + 2a \frac{h}{v} + b \frac{h^2}{v^2} + \dots \right] \quad (4)$$

where in the SM $a = b = 1$, but in composite Higgs theories $\Delta a, \Delta b \sim v^2/\Lambda_{comp}^2$, where Λ_{comp} is the scale of compositeness. Precision measurements of production cross-sections $VV \rightarrow VV$, $VV \rightarrow hh$, and $e^+e^- \rightarrow hZ$ provide sensitivity to the composite scale. The results show that 14 TeV LHC with 100 fb^{-1} of integrated luminosity should have sensitivity of Λ_{comp} up to 7 TeV, 500 GeV LC with 1 ab^{-1} up to 45 TeV, and 3 TeV LC with 1 ab^{-1} up to 60 TeV [11].

4 Additional New Physics

The physics programme of the LC for exploring Terascale physics consists of three broad categories, all of which will be crucial for revealing the possible structure of new physics and for discriminating between different possible manifestations of physics beyond the SM:

- *Refining LHC discoveries:* Phenomena of new physics discovered at the LHC at the time when the LC comes into operation will be probed at the LC in a clean experimental environment and with high precision. This is expected to be decisive for revealing the physics mechanisms behind the observed phenomena.
- *New direct discoveries:* The LC will have a potential for direct discoveries that is complementary to the LHC. In particular, the searches for colour-neutral states of new physics, including the full structure the Higgs sector, will have a discovery potential that far surpasses that of the LHC.
- *Discoveries through precision:* Measurements of observables involving known particles at the LC with the highest possible precision will have a high sensitivity to resolving the fingerprints of new physics, which in many scenarios only manifest themselves in tiny deviations from the SM prediction.

In the following subsections we give examples of new physics where one or more of the above categories of the LC physics programme is on display, some examples of the last having been presented in the earlier discussions of the precision studies in the Higgs, Top and the Gauge sector.

4.1 New Electroweak Matter States

In the BSM context, there are many electroweak states that are well known to be difficult to find directly at the LHC. The event rates at the LHC are small in comparison to strongly interacting particle creation that makes for a challenging background environment.

Of the many ideas that one can use to demonstrate how well new electroweak matter states can be found at a LC, perhaps the most well known is supersymmetry. Supersymmetry provides a good study ground not only because it is a highly motivated scenario for physics beyond the SM, but also because it provides a rather complete and calculable framework beyond the SM with multiple new scalars and fermions of different gauge charges.

The LHC has very good prospects for discovering pair-produced coloured particles up to masses of 2–3 TeV. On the other hand, non-coloured particles, charginos, neutralinos and sleptons are not copiously produced by the LHC. Although these electroweak particles may be found in cascade decays of the production of strongly interacting squarks and gluinos, their prospects for discovery rely on the details of the model. Their accessibility through the decay chains is unlikely to be complete. On the other hand, an e^+e^- collider running at sufficiently high centre-of-mass energy potentially can produce each of these states directly with manageable backgrounds leading to discovery. The discovery reach for these particles produced in pairs at the LC is usually close to $\sqrt{s}/2$, and in some cases even higher if $m_A \neq m_B$ in $e^+e^- \rightarrow AB$ searches.

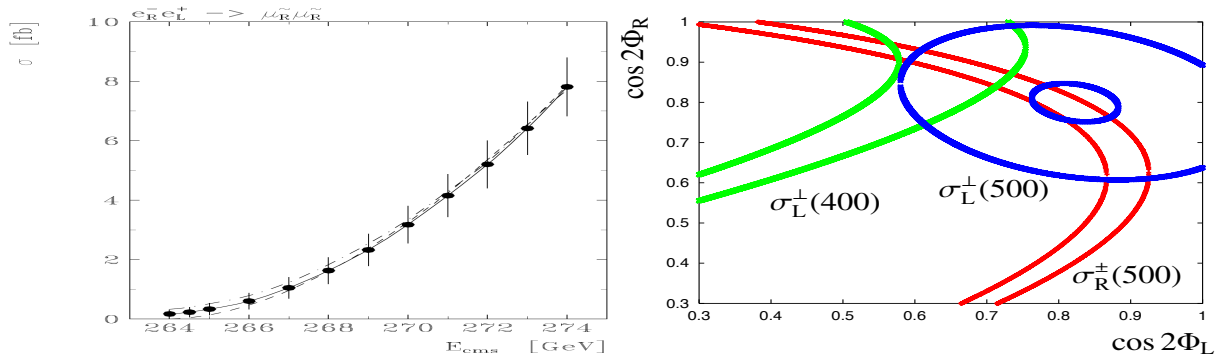


Figure 5: Left: Cross section at threshold for the production of the superpartners of the right-handed muons at the LC, $e^+e^- \rightarrow \tilde{\mu}_R\tilde{\mu}_R$, from which the spin of the produced particles can be determined and their mass can be precisely measured. Right: Determination of the chargino mixing angles $\cos 2\phi_{L,R}$ from LC measurements with polarised beams and at different centre-of-mass energies.

403 The precision studies that are then possible at a LC can test many of the properties of the discovered
 404 particles, such as per mil precise values of their masses and their couplings to SM particles, and assignment
 405 of spins. This can be accomplished through several means, including collecting high integrated luminosity
 406 at high energies and also through threshold scans, which are particular good at measuring the spin due to the
 407 shape of the cross-section versus near-threshold energy, see Figure 5 (left). The precise measurement of the
 408 couplings then enables tests and resolutions of the underlying structure, see Figure 5 (right) for the example
 409 of the determination of the mixing angles between charginos. Detailed measurements of this kind will be
 410 crucial for discriminating a supersymmetric signal from other new physics, since the predictions for the
 411 spins, quantum numbers, couplings and certain mass relations are characteristic features of supersymmetry
 412 that need to be experimentally tested. An example is the ability to test supersymmetry’s equality of fermion
 413 and sfermion (scalar) couplings. Furthermore, the precision measurements of the electroweak superpartner
 414 masses at the LC, combined with the measurements of the masses of the strongly interacting superpartner
 415 masses at the LHC, enable us to test many ideas of the underlying organisational principle for supersym-
 416 metry breaking. Through renormalisation group scaling of well-measured parameters one gets access to the
 417 high-scale (e.g., scale of Grand Unification $\sim 10^{16}$ GeV) structure of the theory, enabling a test of properties
 418 like coupling and mass unification.

419 4.2 Dark Matter

420 It is well established now that the Universe must contain a sizable fraction of cold dark matter. An ideal
 421 candidate for this dark matter is a chargeless massive state χ that interacts with approximately weak gauge
 422 force strength (weakly interacting massive particle, “WIMP”).

423 There are several model-dependent prospects for finding dark matter at the LHC and LC. These include
 424 cascade decays of parent particles that terminate in a stable dark matter particle candidate that carries off
 425 missing energy. These missing energy signature rates depend crucially on many different parameters of the
 426 overarching theory and generally have little to do with the couplings directly relevant to the dark matter
 427 particle itself.

428 On the other hand, a more direct and less model-dependent search for dark matter focusses on the
 429 (effective) $f\bar{f}\chi\chi$ interaction. If the annihilation cross-section is in accordance with the observed relic density,
 430 there are good prospects for the production of dark matter directly at colliders through $f\bar{f} \rightarrow \chi\chi$; however,
 431 since χ leaves no trace in the detector there is no way to directly observe those events. A solution to this
 432 is the related process where an initial state photon or gluon is radiated, which is accessible via the search
 433 for a jet or a photon plus missing energy. The sensitivity of this process at the LHC is limited because

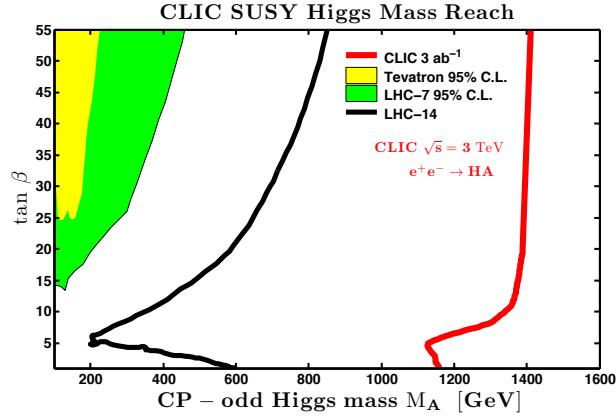


Figure 6: Search reach in the $m_A - \tan\beta$ plane for LHC and for 3 TeV LC. The yellow and green regions are limits already in place from Tevatron and LHC (7 TeV run) analyses. The black line is a 5σ discovery projection for the LHC at 14 TeV with 300fb^{-1} [1] (limits are roughly 150 GeV uniformly higher with 3000fb^{-1}), and the red line is a projection for 3 TeV e^+e^- with 3ab^{-1} of integrated luminosity [11].

434 of significant backgrounds. While at the LHC and in direct detection searches the WIMP interaction with
 435 quarks is probed, the LC provides complementary information on the WIMP interaction with electrons.
 436 Within the clean LC environment, making use of polarised beams, the WIMP mass, the strength and the
 437 chiral structure of the $e^+e^-\chi\chi$ interaction, as well as the dominant partial wave of the production process
 438 can be determined. From the measurements, the WIMP mass and the unpolarised cross-section can be
 439 determined with an accuracy of 0.5–2 GeV and 2–5 fb, respectively, depending on the WIMP properties and
 440 the beam polarisation.

441 LC measurements can also provide a comprehensive set of high-precision experimental information on
 442 the properties of the dark matter particle and the other states affecting annihilation and co-annihilation of
 443 the dark matter particle. This can then be used to predict the dark matter relic density in our Universe. The
 444 comparison of the prediction based on the measurements of new physics states at the LHC and the LC with
 445 the precise measurement of the relic density from cosmological data would constitute an excellent test of
 446 the dark matter hypothesis.

447 4.3 Additional Higgs Bosons

448 After the confirmation of the existence of a state compatible with the SM Higgs boson, there is still the
 449 prospect of additional Higgs bosons in the spectrum. These additional Higgs bosons include extra singlet
 450 Higgs bosons that mix with the SM-type Higgs boson. Or, there may be an extra $SU(2)_L$ doublet that fills
 451 out the full Higgs sector of the theory.

452 Again, supersymmetry provides an excellent, calculable framework through which to analyze the dis-
 453 covery prospects of an extra Higgs boson. Over a large part of the parameter space the Higgs sector consists
 454 of one light state ($m_h \lesssim 135\text{ GeV}$) whose couplings are very similar to the SM Higgs boson, and four extra
 455 states (A^0 , H^0 and H^\pm) of nearly equal mass. Figure 6 shows the direct discovery reach of the heavy Higgs
 456 bosons at the LHC and a 3 TeV LC as a function of m_A . The result is impressive, with a search capacity
 457 for the heavy Higgs near $\sqrt{s}/2$ for the LC. If the dark matter particle has less than half the mass of a Higgs
 458 boson, invisible Higgs decays could be another source for producing dark matter. This possibility can be
 459 studied in detail at the LC for all Higgs bosons within its kinematic reach.

460 An extended Higgs sector could also contain a light Higgs, possibly in addition to a SM-like Higgs at
 461 about 125 GeV, with a mass below the LEP limit of about 114 GeV and with suppressed couplings to gauge
 462 bosons. While at the LHC the search for such a light Higgs state will be very challenging in the standard

463 search channels, at the LC there will be a high sensitivity for probing scenarios of this kind.

464 **4.4 New Gauge Boson Interactions**

465 The quintessential example of a new gauge boson is a Z' boson. The mass reach for direct discovery at
466 the LHC of an “ordinary” Z' boson, whose couplings to the SM fermions are $\mathcal{O}(1)$, is generally about
467 5 TeV. However, it is well documented that through non-resonance observables an e^+e^- collider with energy
468 above a few hundred GeV has an even higher reach for detecting BSM signals. This is accomplished by
469 studying precisely the observables of the $e^+e^- \rightarrow f\bar{f}$ processes. Small deviations in $\sigma_{\text{tot}}^{\text{ff}}$, A_{FB}^f and A_{LR}^f can
470 be found for Z' masses well above the centre-of-mass energy of the machine. For example, at a 500 GeV
471 LC with 1 ab^{-1} of integrated luminosity, a BSM signal is detectable in the left-right model (i.e., theory with
472 $\text{SU}(2)_{\text{R}} \times \text{U}(1)_{\text{B-L}} \rightarrow \text{U}(1)_{\text{Y}}$) if the corresponding Z' has a mass below 9 TeV, which is more than one order
473 of magnitude beyond the centre-of-mass energy of the collider. This search reach increases to about 16 TeV
474 at a 1 TeV LC (see sec. 5.2.1 of [2]) and to well beyond 30 TeV for a 3 TeV LC (see sec. 1.5 of [11]).

475 **4.5 Model-Independent Searches**

476 Some of the discussion above has revolved around specific model scenarios. However, it must be empha-
477 sised that the LC is an excellent machine to do model-independent analyses in the context of the uniquely
478 clean e^+e^- collision environment. Searches can be made to test whether the event rates in different chan-
479 nels are anomalous, and thus indicate the presence of new physics. We have already mentioned above an
480 analysis of dark matter production at the LC with little model dependence, and the excellent prospects for
481 discovery if kinematically accessible. A minimum number of theoretical assumptions are necessary to de-
482 termine the spin, mass and couplings of new particles, which can then be used in a second step to obtain
483 theoretical interpretations in different models. Thus, instead of referring to a particular class of models,
484 like the discussion above of Z' effects suppressed by $M_{Z'}$, one can also interpret the LC results in terms of
485 general effective operators, such as non-renormalizable contact operators suppressed by a scale Λ . These
486 more general interpretations of the LC sensitivities may not always be stated explicitly since many studies
487 have been carried out within a well-defined BSM model, but it is an advantageous feature of the LC that
488 such model-independent interpretations are possible.

489 With the so-called GigaZ option of the LC, i.e. a run at the Z peak with polarised e^- and e^+ beams col-
490 lecting about 10^9 events, the LC can provide high-precision measurements that have a very high sensitivity
491 to effects of new physics, which are probed in a model-independent way. In particular, the GigaZ run would
492 reduce the present experimental uncertainties on the effective weak mixing angle, $\sin^2 \theta_{\text{eff}}$, by more than an
493 order of magnitude, and resolve or confirm the significant (3σ) disagreement between the two most precise
494 determinations of $\sin^2 \theta_{\text{eff}}$ from A_{FB}^b at LEP and A_{LR} at SLC. As an example, the precision achievable for
495 $\sin^2 \theta_{\text{eff}}$ at GigaZ has the potential to reveal the impact of new physics even in a scenario where no states of
496 physics beyond the SM would be observed at the LHC and the first phase of a LC.

497 **Executive Summary**

498 The observation at the LHC of a SM-like Higgs particle provides the first direct test of the minimal SM
499 EWSB scenario of a single scalar doublet Higgs field producing the vacuum expectation value. Having
500 made this discovery the physics case for a LC is extraordinarily strong. The LC provides the capability to
501 study the details of this new form of matter, establishing agreement with the SM predictions to new levels
502 of sensitivity, or revealing a break from the patterns expected in the SM. The precision of the LC opens
503 sensitivity to new physics well beyond the LC’s direct reach, enabling detection before discovery, such as
504 past indirect evidence for the Higgs boson, the top quark, the charm quark, and the weak gauge bosons.

505 The most powerful and unique property of the LC is its flexibility. It can be tuned to well-defined
506 initial states, including polarisation, allowing numerous model-independent measurements, from the Higgs

507 threshold to multi-TeV operation, as well as the possibility of unprecedented precision at the Z-pole (GigaZ).
508 Furthermore, the relative simplicity of the production processes and final state configurations makes com-
509 plete and extremely accurate reconstruction and measurement possible. The envisioned physics programme
510 includes precision measurements of many Higgs decay widths, some of which are uniquely accessible at the
511 LC ($c\bar{c}$, gg , the invisible mode and the full width), decisive tests of the spin-parity properties of the Higgs
512 candidate, and determinations of the top-Higgs and trilinear Higgs self couplings, also uniquely accessible
513 at the LC. For a LC operating up to and beyond 500 GeV, the complete SM, including Higgs, top quark and
514 VV interactions can be studied, both at tree level and through quantum corrections. In addition to precision
515 tests of minimal EWSB and its Higgs boson(s), the LC also reaches well into new physics territory, where
516 the potential exists to discover dark matter, aspects of supersymmetry, evidence for composite Higgs, or to
517 test other well motivated BSM ideas. The physics reach of the LC is essentially limited by statistics, not
518 systematics. Its discovery reach exceeds that of the LHC at any integrated luminosity in many cases, and
519 discoveries of new particles or interactions at either machine can be subjected to further precision analysis
520 at the LC to reveal deeper structures of nature.

521 **References**

- 522 [1] F. Gianotti, *et al.*, *Physics potential and experimental challenges of the LHC luminosity upgrade* Eur.
523 Phys. J. C39 (2005) 293.
- 524 [2] J. A. Aguilar-Saavedra *et al.* [ECFA/DESY LC Physics Working Group Collaboration], “*TESLA: Tech-*
525 *nical design report. Part 3. Physics at an e^+e^- linear collider,*” hep-ph/0106315.
- 526 [3] T. Abe *et al.* [American Linear Collider Working Group Collaboration], *Linear collider physics re-*
527 *source book for Snowmass 2001*, hep-ex/0106055, SLAC-R-570.
- 528 [4] K. Abe *et al.* [ACFA Linear Collider Working Group Collaboration], *Particle physics experiments at*
529 *JLC*, hep-ph/0109166.
- 530 [5] G. Weiglein *et al.* [LHC/LC Study Group Collaboration], *Physics interplay of the LHC and the ILC*,
531 Phys. Rept. **426** (2006) 47 [hep-ph/0410364].
- 532 [6] E. Accomando *et al.* [CLIC Physics Working Group Collaboration], “*Physics at the CLIC multi-TeV*
533 *linear collider,*” hep-ph/0412251.
- 534 [7] G. Moortgat-Pick *et al.*, *The Role of polarized positrons and electrons in revealing fundamental inter-*
535 *actions at the linear collider*, Phys. Rept. **460** (2008) 131 [hep-ph/0507011].
- 536 [8] G. Aarons *et al.* [ILC Global Design Effort and World Wide Study], “*International Linear Collider*
537 *Reference Design Report Volume 2: Physics at the ILC,*” arXiv:0709.1893 [hep-ph].
- 538 [9] H. Aihara *et al.* [SiD Concept Group], “*SiD Letter of Intent,*” arXiv:0911.0006 [physics.ins-det].
- 539 [10] T. Abe *et al.* [ILD Concept Group], “*The International Large Detector: Letter of Intent,*”
540 arXiv:1006.3396 [hep-ex].
- 541 [11] L. Linssen *et al.* [CLIC Working Groups], “*Physics and Detectors at CLIC: CLIC Conceptual Design*
542 *Report,*” arXiv:1202.5940 [physics.ins-det].
- 543 [12] E. Accomando *et al.*, “*Workshop on CP Studies and Non-Standard Higgs Physics,*” hep-ph/0608079.
- 544 [13] T. Barklow, *et al.*, “*Physics at the International Linear Collider,*” to be published as a chapter of the
545 *ILC Detailed Baseline Design Report* (2012).

546 **Addendum: Charge for the Linear Collider Report Committee**

547 During the international Linear Collider Workshop in Granada October 2011 it was proposed and agreed
548 to charge a small expert group with drafting a common Linear Collider Physics report to be submitted as
549 input to the European Strategy process. The initiative was presented in Granada by the GDE European
550 Regional Director (Brian Foster), the CERN Linear Collider Studies Leader (Steinar Stapnes) and the Chair
551 of the ECFA Study for the Linear Collider (Juan Fuster), and was a result of discussions and consensus in
552 several ILC and CLIC steering committee meetings earlier in 2011. These three subsequently suggested a
553 composition of the expert committee based on input from the community, and proposed the mandate of the
554 committee. The draft report has been through internal reviews, and has been made openly available to the
555 full international LC community for further comments and suggestions before submission by end of July
556 2012.

557 *Mandate of the committee:*

558 The committee is requested to review the physics case for a linear electron-positron collider in the
559 centre-of-mass energy range from around 250 GeV – 3 TeV in the light of LHC results up to mid-2012 and
560 building on previous studies. The committee should consider the case for a linear collider in terms of the
561 physics reach beyond that of the LHC under the assumptions in the current CERN planning; a) 300 fb⁻¹ and
562 b) 3000 fb⁻¹.

563 It should assume linear collider performance based on the details contained in current documents from
564 ILC and CLIC but without a detailed comparison of the relative performance of the machines. The aim is
565 to make the strongest possible case for a generic linear collider for submission to the European Strategy
566 process.

567 The committee is requested to submit its draft report to the GDE European Regional Director, the CERN
568 Linear Collider Studies Leader and the Chair of the ECFA Study for the Linear Collider by June 18th 2012.
569 The final version of the report should be delivered by end of July 2012.